

Hadronic light-by-light scattering contributions to $(g - 2)_\mu$ from axial-vector and tensor mesons in the holographic soft-wall model

Pietro Colangelo^{✉,*}, Floriana Giannuzzi^{✉,†} and Stefano Nicotri^{✉,‡}

INFN—Istituto Nazionale di Fisica Nucleare—Sezione di Bari Via Orabona 4, 70125, Bari, Italy



(Received 16 February 2024; accepted 6 May 2024; published 23 May 2024)

We compute the light axial-vector and tensor meson two-photon transition form factors in the soft-wall holographic model of quantum chromodynamics (QCD) in the flavor-symmetric case. They are used to evaluate the axial-vector and tensor meson contributions to the anomalous magnetic moment of the muon via the hadronic light-by-light scattering process. As expected, these contributions are smaller than the one from pseudoscalar mesons. The result for axial-vector mesons is higher than the value found in other approaches.

DOI: [10.1103/PhysRevD.109.094036](https://doi.org/10.1103/PhysRevD.109.094036)

I. INTRODUCTION

One of the most interesting observables currently under investigation is the anomalous magnetic moment of the muon, $a_\mu = (g_\mu - 2)/2$, which is challenging the Standard Model (SM) of fundamental interactions. The puzzle deals with the current tension between the measurements [1] and a SM prediction [2]. The most precise measurement has been recently provided by the Muon $g - 2$ experiment at Fermilab [1], which has improved the precision of the experimental world average by a factor of 2. From the theoretical point of view, a comprehensive prediction for the SM value has been presented in the white paper of the Muon $g - 2$ Theory Initiative in 2020 [2]. The Fermilab result and the expectation quoted in Ref. [2] deviate at a level of about 5σ . Considering all available data a smaller discrepancy is found [1].

In the SM the largest contribution to a_μ comes from QED processes, and is very precisely known. Electroweak corrections have also been precisely determined [3]. Then, two kinds of QCD contributions are involved: the leading one corresponds to the hadronic vacuum polarization (HVP) [4], the subleading one is due to hadronic light-by-light scattering (HLbL) [5]. New discussions can be found in [6].

QCD contributions are the most interesting to look at, since the theoretical uncertainty is dominated by hadronic

effects. A tension exists between the HVP contribution computed from the $e^+e^- \rightarrow \text{hadrons}$ cross section data, used in [2], and the lattice QCD result obtained by the BMW collaboration [7]. If the latter value is used to obtain the SM a_μ , the discrepancy with the experimental result is reduced to 1.6σ [8]. Moreover, there is a discrepancy between the measurements of the $e^+e^- \rightarrow \pi^+\pi^-$ cross section obtained from the BABAR [9] and KLOE [10] collaborations. In this respect, a recent determination by the CMD-3 collaboration [11] is larger than the previous measurements in the energy range up to $\sqrt{s} \simeq 1.2$ GeV. The latter value would increase the HVP contribution determined in [2], reducing the tension between the experimental value of a_μ and the SM expectation. On the other hand, the confirmation of the discrepancy between experimental and theoretical values of a_μ by forthcoming data and theoretical studies would open exciting perspectives for revealing new physics effects [12].

The theoretical prediction of the HLbL contribution needs to be improved as well in order to meet the precision of 16×10^{-11} for a_μ projected for the Fermilab experiment [13]. The HLbL contribution has been computed in a series of studies summarized in Ref. [2] using a dispersive approach. This allows a model-independent evaluation but fails in reproducing short-distance constraints (SDCs) [14], an issue that has been debated in recent years [15–17], so a strategy should be found in order to incorporate them. The dominant contribution comes from the poles of the light pseudoscalar mesons. The contributions from other states (scalar, tensor and axial-vector states) are smaller, but need to be computed to improve the theoretical accuracy.

In this paper we compute the axial-vector and tensor meson contributions to the HLbL term in the soft-wall model, a QCD phenomenological holographic approach briefly described in Section II [18]. Axial-vector mesons

*pietro.colangelo@ba.infn.it

†floriana.giannuzzi@ba.infn.it

‡nicotri@infn.it

Published by the American Physical Society under the terms of the [Creative Commons Attribution 4.0 International license](https://creativecommons.org/licenses/by/4.0/). Further distribution of this work must maintain attribution to the author(s) and the published article's title, journal citation, and DOI. Funded by SCOAP³.

play an essential role since they are expected to solve the SDC puzzle reproducing the correct large- Q^2 behavior of the longitudinal four-point function. In this respect, holographic computations in the hard-wall model with different mechanisms of breaking chiral symmetry have proven to be useful in providing an analytical tool for computing the relevant four-point functions, showing how the sum over the infinite tower of axial-vector states can give the expected result [19,20]. This is discussed in Sec. III.

Tensor meson contributions are expected to be smaller than contributions from pseudoscalar exchange. However, in view of improving the theoretical precision it is important to correctly estimate this contribution, for which there are only a few theoretical studies. We compute it by studying the two-photon transition form factor for the helicity-2 meson component in the holographic soft-wall model, obtaining an analytic expression as a function of the photon virtualities. The computation is presented in Sec. IV, with a few technical details collected in the Appendix A and B.

II. THE SOFT-WALL MODEL

The soft-wall (SW) holographic model of QCD is defined in the 5D space with background anti-de Sitter (AdS) geometry, the bulk, with line element

$$ds^2 = g_{MN} dx^M dx^N = \frac{R^2}{z^2} (\eta_{\mu\nu} dx^\mu dx^\nu - dz^2). \quad (1)$$

R is the radius of curvature of the AdS space and $\eta_{\mu\nu} = \text{diag}(1, -1, -1, -1)$. We use Greek letters for Minkowski (4D) indices, and capital letters for AdS (5D) indices. The fifth z (bulk) coordinate runs in the range $\varepsilon < z < \infty$ with ε a small ($\varepsilon \rightarrow 0$) positive UV cutoff. The defining feature of the model is a background (i.e. nondynamical) dilaton field $\phi(z)$ which only depends on the bulk coordinate z and appears in the Lagrangian as $e^{-\phi(z)}$ [18]. A minimal choice is $\phi(z) = c^2 z^2$, where the dimensionful constant c , linked to Λ_{QCD} , breaks conformal invariance and is responsible for color confinement. Such a choice for $\phi(z)$ allows to recover linear Regge trajectories for the spectra of light vector mesons [18], light scalar mesons [21], 0^{++} and 0^{--} glueballs [22,23], and 1^{-+} hybrid mesons [24]. According to the AdS/CFT dictionary, the global $U(n_f)_L \times U(n_f)_R$ symmetry of QCD is dual to a local (gauge) symmetry in the 5D theory, where the fields dual to the QCD left- and right-handed currents $\bar{q}_{L/R} \gamma^\mu T^a q_{L/R}$ are the massless 1-forms $B_L(x, z)$ and $B_R(x, z)$.¹ Such gauge fields are expressed as $B_{\{L,R\}}^M(x, z) = B_{\{L,R\}}^{M,a}(x, z) T^a$, where $T^a = \lambda^a/2$ ($a = 0, \dots, n_f^2 - 1$) are the generators

¹The relation between the 5D mass of a p -form and the conformal dimension Δ of its dual 4D operator is $m_5^2 R^2 = (\Delta - p)(\Delta + p - 4)$, for a spin 2 it is $m_5^2 R^2 = \Delta(\Delta - 4)$ [25].

of $U(n_f)$, with $T^0 = \frac{1}{\sqrt{2n_f}} \mathbb{1}_{n_f}$ ($\mathbb{1}_{n_f}$ is the $n_f \times n_f$ identity matrix), and $\text{Tr}(T^a T^b) = \delta^{ab}/2$ for $a, b = 0, \dots, n_f^2 - 1$. Vector and axial-vector fields are defined as $V = (B_L + B_R)/2$ and $A = (B_L - B_R)/2$, respectively. The $\bar{q}_R q_L$ operator is dual to a tachyon field $X(x, z) = X_0(z) e^{i\pi^a(x,z)T^a}$, π^a describing the nonet of pseudoscalar mesons and X_0 parametrized as $X_0(z) = \sqrt{2}v(z)\mathbb{1}_{n_f}$. We consider the case of $n_f = 3$ light quarks. The covariant derivative acts on $X(x, z)$ as

$$D_M X = \partial_M X + i[X, V_M] - i\{X, A_M\}. \quad (2)$$

III. AXIAL-VECTOR MESON CONTRIBUTION TO a_μ^{HLbL}

The quadratic action for the axial-vector field $A_M(x, z)$ is [18]

$$S_A = \frac{R}{k} \int d^5 x e^{-c^2 z^2} \left(-\frac{1}{4g_5^2 z} F^a F^a + \frac{4v(z)^2}{z^3} (\partial\pi^a - A^a)^2 \right), \quad (3)$$

where $F_{MN} = \partial_M A_N - \partial_N A_M$. The prefactors $R/k = N_c/16\pi^2$ and $g_5^2 = 3/4$ are fixed by matching the two-point correlation functions of the vector and scalar quark currents to the perturbative QCD expressions [22]. We set the AdS radius $R = 1$.

The coupling of the axial field to two vector fields, contributing to $(g-2)_\mu$, is provided by the Chern-Simons action [26–28]

$$S_{CS} = S_{CS}^L - S_{CS}^R \quad (4)$$

where

$$S_{CS}^{L/R} = \frac{N_c}{24\pi^2} \int \text{Tr} \left(\mathcal{B} \mathcal{F}^2 - \frac{i}{2} \mathcal{B}^3 \mathcal{F} - \frac{1}{10} \mathcal{B}^5 \right), \quad (5)$$

$\mathcal{B} = B_M dx^M$ and $\mathcal{F} = (\partial_A B_B) dx^A \wedge dx^B$. We emphasize that, differently from Ref. [28], we are considering a flavor-symmetric model, and we are not including terms related to the $U(1)_A$ anomaly. In the gauge $B_z = 0$ and keeping only VVA terms, we find, as in the hard-wall model [20],

$$S_{CS} = -\frac{N_c}{6\pi^2} \text{Tr} (Q_{em}^2 T^a) \varepsilon^{\mu\beta\gamma\delta} \int d^5 x (3(\partial_z V_\beta)(\partial_\gamma V_\delta) A_\mu^a + \partial_z (A_\beta^a (\partial_\gamma V_\delta) V_\mu)). \quad (6)$$

V_μ is the electromagnetic field, proportional to the light-quark electromagnetic charge matrix Q_{em} and dual to the electromagnetic current.

A_μ can be split in a transverse and a longitudinal component: $A_\mu^a = A_\mu^{a\perp} + \partial_\mu \varphi^a$. The longitudinal component of the axial-vector field (φ^a) mixes with the field π^a dual to the pseudoscalar current, and they describe pseudoscalar mesons. The equations of motion for the transverse and longitudinal components of the axial-vector field come from the quadratic action (3) and in the Fourier space they read:

$$\partial_z \left(\frac{e^{-\phi(z)}}{z} \partial_z A_\mu^{a\perp}(z) \right) + q^2 \frac{e^{-\phi(z)}}{z} A_\mu^{a\perp}(z) - \frac{8g_5^2 v(z)^2 e^{-\phi(z)}}{z^3} A_\mu^{a\perp}(z) = 0 \quad (7)$$

$$\partial_z \left(\frac{e^{-\phi(z)}}{z} \partial_z \varphi^a(z) \right) + \frac{8g_5^2 v(z)^2 e^{-\phi(z)}}{z^3} (\pi^a(z) - \varphi^a(z)) = 0 \quad (8)$$

$$\partial_z \left(\frac{e^{-\phi(z)} v(z)^2}{z^3} \partial_z \pi^a(z) \right) + \frac{e^{-\phi(z)} v(z)^2}{z^3} q^2 (\pi^a(z) - \varphi^a(z)) = 0. \quad (9)$$

The eigenvalues $q^2 = m_n^2$ for the transverse component are found requiring $A_n^{a\perp}(0) = 0$ and $\partial_z A_n^{a\perp}(z) = 0$ for $z \rightarrow \infty$, and the eigenfunction normalization condition is

$$\frac{R}{kg_5^2} \int_0^\infty dz \frac{e^{-\phi(z)}}{z} A_n^{a\perp}(z)^2 = 1. \quad (10)$$

If we use

$$v(z) = m_q z + \sigma z^3, \quad (11)$$

with $m_q = 3.47$ MeV, $\sigma = 0.149$ GeV³ and $c = 0.388$ GeV, fixed from the pion mass, the pion decay constant and the ρ mass [28], respectively, we find $m_0 = 1.679$ GeV for the ground-state mass. In this flavor-symmetric model, m_q is matched to the up and down quark mass. The axial-vector decay constant, defined as

$$\langle 0 | \bar{q} \gamma_\mu \gamma_5 T^a q | A_n \rangle = f_n^a m_n \varepsilon_\mu, \quad (12)$$

can be computed from the expression

$$f_n^a = \frac{R}{kg_5^2} \frac{1}{m_n} \lim_{z \rightarrow 0} \frac{e^{-\phi(z)}}{z} \partial_z A_n^{a\perp}(z). \quad (13)$$

For the ground state we find $f_0^a = 221$ MeV. These results are independent of the flavor index a .

The contribution to muon $g - 2$ from the longitudinal component of the axial-vector field in the soft-wall model has been analyzed in [28], where the η' meson has been

included considering the mixing between pseudoscalar mesons and pseudoscalar glueballs [29].

Let us compute the contribution of axial-vector mesons (transverse component) to the correlation function of four vector currents, the $\Pi_{\mu\nu\lambda\sigma}^A$ tensor. As in Ref. [20], we consider it as the sum of the product of two three-point amplitudes times a propagator over all intermediate axial-vector states [30]:

$$\begin{aligned} & \Pi_{\mu\nu\lambda\sigma}^A(q_1, q_2, q_3, q_4) \\ &= M_{\mu\nu\alpha}(q_1, q_2) \frac{iP^{\alpha\beta}(q_3 + q_4)}{(q_3 + q_4)^2 - M_A^2} M_{\lambda\sigma\beta}(q_3, q_4) \\ &+ M_{\mu\sigma\alpha}(q_1, q_4) \frac{iP^{\alpha\beta}(q_1 + q_4)}{(q_1 + q_4)^2 - M_A^2} M_{\nu\lambda\beta}(q_2, q_3) \\ &+ M_{\mu\lambda\alpha}(q_1, q_3) \frac{iP^{\alpha\beta}(q_1 + q_3)}{(q_1 + q_3)^2 - M_A^2} M_{\nu\sigma\beta}(q_2, q_4), \end{aligned} \quad (14)$$

where M_A is the mass of the axial-vector meson, $P_{\mu\nu} = \eta_{\mu\nu} - \frac{q_\mu q_\nu}{M_A^2}$ is the projector for spin 1 mesons, and q_1, q_2, q_3, q_4 are the momenta of the incoming photons.

Following [20,30], the amplitude $\gamma^* \gamma^* \rightarrow A_n^a$ is written as

$$\begin{aligned} M_{\mu\nu\alpha}(q_1, q_2) &= e^2 \varepsilon_{\rho\nu\alpha\tau} (q_1^\tau g_\mu^\rho - q_1^\rho q_{1\mu}) q_2^\tau F_{A_n^* \gamma^*}(q_1^2, q_2^2) \\ &- e^2 \varepsilon_{\mu\rho\alpha\tau} (q_2^\tau g_\nu^\rho - q_2^\rho q_{2\nu}) q_1^\tau F_{A_n^* \gamma^*}(q_2^2, q_1^2) \end{aligned} \quad (15)$$

where $F_{A_n^* \gamma^*}$ is the two-photon transition form factor (TFF).² In the soft-wall model the three-point function of an axial-vector current and two vector currents is obtained from the Chern-Simons action (6). The eigenfunctions $A_n^{a\perp}(z)$ vanish both at $z = 0$ and for $z \rightarrow \infty$, so the last term in Eq. (6) does not contribute. Then, the TFF of the axial-vector meson $A_n^{a\perp}$ to two photons is given by [20]:

$$\begin{aligned} F_{A_n^* \gamma^*}(Q_1^2, Q_2^2) &= \frac{N_c}{4\pi^2} \text{Tr}(Q_{em}^2 T^a) \frac{2}{Q_1^2} \int_0^\infty dz A_n^{a\perp}(z) \\ &\times \partial_z V(z, Q_1^2) V(z, Q_2^2), \end{aligned} \quad (16)$$

where $Q_i^2 = -q_i^2$ and $V(z, Q^2)$ is the bulk-to-boundary propagator (BTBP) of the vector field

$$V(z, Q^2) = \frac{Q^2}{4c^2} \Gamma\left(\frac{Q^2}{4c^2}\right) U\left(\frac{Q^2}{4c^2}, 0, c^2 z^2\right), \quad (17)$$

²In general, for axial-vector mesons three form factors appear in the decomposition of $M_{\mu\nu\alpha}(q_1, q_2)$ [31], while in the holographic model one obtains the amplitude as in Eq. (15) involving only two form factors. The origin of this mismatch is currently under investigation.

with U the Tricomi confluent hypergeometric function [18,27]. In the model the light quark masses coincide and we do not distinguish among mesons with $a = 3, 8, 0$. In the TFF the only difference between the states is in the factor $\text{Tr}(Q_{em}^2 T^a)$. We find that the form factors of the lowest-lying axial-vector mesons with $a = 8, 0$ to two real photons are $F_{A_0^8 \gamma \gamma} = -0.170 \text{ GeV}^{-2}$ and $F_{A_0^0 \gamma \gamma} = -0.480 \text{ GeV}^{-2}$. The amplitude for the decay in two real photons vanishes, satisfying the Landau-Yang theorem. An equivalent two-photon decay width for an axial-vector meson to decay in one quasireal longitudinal photon and a real photon can be defined as [32]

$$\tilde{\Gamma}_{A_0^a \rightarrow \gamma \gamma} = \lim_{Q_1^2 \rightarrow 0} \frac{m_0^2}{Q_1^2} \frac{1}{2} \Gamma_{A_0^a \rightarrow \gamma^* \gamma} = \frac{\pi \alpha^2 m_0^5}{12} F_{A_0^a \gamma \gamma}^2, \quad (18)$$

where Q_1^2 is the virtuality of the photon γ^* . We find $\tilde{\Gamma}_{A_0^8 \gamma \gamma} = 5.4 \text{ keV}$ and $\tilde{\Gamma}_{A_0^0 \gamma \gamma} = 43 \text{ keV}$. In the hard-wall (HW) model $F_{A_0^8 \gamma \gamma} = -0.154 \text{ GeV}^{-2}$ and $F_{A_0^0 \gamma \gamma} = -0.435 \text{ GeV}^{-2}$ have been found [20]. Experimental data for $f_1(1285)$ and $f_1(1420)$ are: $\tilde{\Gamma}_{\gamma \gamma} = 3.5(8) \text{ keV}$ for $f_1(1285)$ [33] and $\tilde{\Gamma}_{\gamma \gamma} = 3.2(9) \text{ keV}$ for $f_1(1420)$ [34].

Figure 1 shows the Q^2 dependence of the axial-vector TFF with one real photon compared to the result in the hard-wall model [20] and to the dipole parametrization of Ref. [30]

$$\frac{F_{A\gamma\gamma}(Q_1^2, Q_2^2)}{F_{A\gamma\gamma}(0, 0)} = \frac{1}{(1 + Q_1^2/\Lambda^2)^2} \frac{1}{(1 + Q_2^2/\Lambda^2)^2} \quad (19)$$

with $\Lambda = 1040 \pm 78 \text{ MeV}$ determined from phenomenology for $f_1(1285)$ [33]. A similar plot is shown in Fig. 2 for

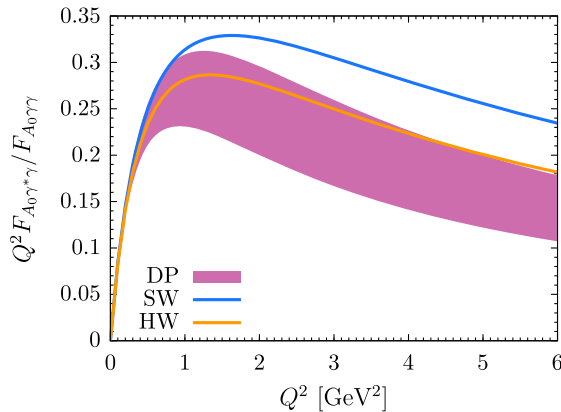


FIG. 1. Axial-vector two-photon transition form factor for one real photon. The blue curve (SW) shows the result obtained in the soft-wall model; the orange curve (HW) shows the result obtained in the hard-wall model with bi-fundamental scalar, denoted as HW1 in [20]; the magenta band shows the dipole-parametrization expression (DP) in Eq. (19) including the uncertainty on the parameter Λ .

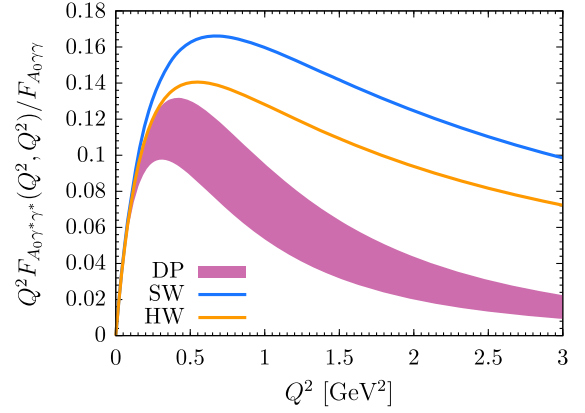


FIG. 2. Axial-vector transition form factor for two virtual photons. Line colors are the same as in Fig. 1.

$F_{A_0^a \gamma^* \gamma^*}(Q^2, Q^2)$. The high- Q^2 behavior in the holographic models is the same as in the dipole parametrization for the TFF with one real photon. For two virtual photons the holographic models still find a Q^{-4} decrease of the TFF, while the parametrization in [30] produces a Q^{-8} decrease. As noticed in [20,35], defining $Q^2 = (Q_1^2 + Q_2^2)/2$ and $w = (Q_1^2 - Q_2^2)/(Q_1^2 + Q_2^2)$, the asymptotic behavior of the axial-vector TFF for $Q^2 \rightarrow \infty$ in both the soft-wall and hard-wall models is

$$\begin{aligned} F_{A_0^a \gamma^* \gamma^*}(Q_1^2, Q_2^2) &\xrightarrow{Q^2 \rightarrow \infty} -N_c \text{Tr}(Q_{em}^2 T^a) \frac{f_0^a m_0}{Q^4} \sqrt{1-w} \\ &\times \int_0^\infty dx x^4 K_0(x\sqrt{1+w}) K_1(x\sqrt{1-w}) \\ &= -N_c \text{Tr}(Q_{em}^2 T^a) \frac{f_0^a m_0}{Q^4 w^4} \left(w(3-2w) \right. \\ &\left. + \frac{1}{2}(w+3)(1-w) \log \frac{1-w}{1+w} \right), \quad (20) \end{aligned}$$

a result which agrees with the expansion in [36]. $K_n(x)$ is the modified Bessel function of the second kind. The hard-wall and soft-wall models give the same result in this limit since the leading behavior of vector meson BTBP in both models is $V(z, Q^2) = z\sqrt{Q^2} K_1(z\sqrt{Q^2})$ [27]. To obtain Eq. (20) we have used the expansion of the axial wave function at small z and the definition of the axial-vector decay constant f_0^a in (13):

$$A_0^{a\perp}(z) \xrightarrow{z \rightarrow 0} \left(\frac{R}{kg_5^2} \right)^{-1} \frac{f_0^a m_0}{2} z^2. \quad (21)$$

The hadronic light-by-light (HLbL) pole contribution from axial-vector mesons to $(g-2)_\mu$ can be computed from

$$a_\mu^{HLbL} = \int_0^\infty dQ_1 \int_0^\infty dQ_2 \int_{-1}^1 d\tau \rho_a(Q_1, Q_2, \tau), \quad (22)$$

TABLE I. HLbL contribution to $a_\mu (\times 10^{11})$ of the axial-vector mesons a_1, f_1, f'_1 in the indicated references. For more results see Table 13 in [2]. All values refer to the ground states, with the exception of the one quoted as Ref. [19] corresponding to the whole meson tower. In [20] the same model (called HW2) of Ref. [19] is considered, with flavor-symmetric normalizations, and the ground state contributions are 80% of the whole meson tower.

Ref.	a_1^0	$f_1(1285)$	$f'_1(1420)$	Sum
White Paper [2]				6 ± 6
Bijnens <i>et al.</i> [37]				2.5 ± 1
Hayakawa <i>et al.</i> [38]				1.738 ± 0.003
Melnikov <i>et al.</i> [14]	5.7	15.6	0.8	22 ± 5
Pauk <i>et al.</i> [30]		5.0 ± 2.0	1.4 ± 0.7	6.4 ± 2.0
Roig <i>et al.</i> [31]	0.21 ± 0.04	0.58 ± 0.11	0.015 ± 0.008	$0.8^{+3.5}_{-0.8}$
Leutgeb <i>et al.</i> [20,35]				29.8–33.2
Cappiello <i>et al.</i> [19]	8	8	12	28
Masjuan <i>et al.</i> [15]	5.89	10.52	1.97	18.38
Leutgeb <i>et al.</i> [39]	7.1–7.8	4.3–5.7	13.6–14.3	25.0–27.8
Radzhabov <i>et al.</i> [40]				3.6 ± 1.8
This work				36

where ρ_a is defined in the appendix of Ref. [20]. We find $a_{\mu, A^3}^{HLbL} = 9.0 \times 10^{-11}$, $a_{\mu, A^8}^{HLbL} = 3.0 \times 10^{-11}$, $a_{\mu, A^0}^{HLbL} = 24 \times 10^{-11}$ [the difference is only due to the factor $\text{Tr}(Q_{em}^2 T^a)$], the sum being $a_\mu^{HLbL} = 36 \times 10^{-11}$. In Table I other determinations are collected, showing that a large uncertainty affects the size of this contribution. The soft-wall model, as well as the hard-wall model [20], points toward high values. Indeed, it has been noticed [14,15] that higher a_μ from axial-vector mesons are found in models able to reproduce the SDCs on the longitudinal four-point function.

Notice that, as stated in Ref. [30], when calculating a_μ^{HLbL} the sum over polarizations of spin-1 particles gives the projector $P_{\mu\nu} = \eta_{\mu\nu} - \frac{q_\mu q_\nu}{M_A^2}$, containing both transverse and longitudinal contributions. We can separate them as the sum of a transverse $P_{\mu\nu}^\perp = \eta_{\mu\nu} - \frac{q_\mu q_\nu}{q^2}$ and a longitudinal projector $P_{\mu\nu}^\parallel = \frac{q_\mu q_\nu}{q^2} - \frac{M_A^2 - q^2}{M_A^2}$. Using the transverse projector, we find $a_\mu^{HLbL, \perp} = 16 \times 10^{-11}$, and using the longitudinal one we find $a_\mu^{HLbL, \parallel} = 20 \times 10^{-11}$, both values including the contributions from $a = 3, 8, 0$.

The contributions from the excited states are smaller. Even though the soft-wall model is not able to correctly

describe these states in the axial-vector sector, we have computed their contributions to a_μ^{HLbL} with the results collected in the Table II. Moreover, following [20], we have computed the Green's function of the axial-vector field and used it to determine the contribution to a_μ^{HLbL} from the whole tower of axial-vector mesons. We find $a_\mu^{HLbL} = 41.3(18.1 + 23.2) \times 10^{-11}$, with the values in parentheses corresponding to the transverse and longitudinal contributions. This value is included also in Table II, last column. This result agrees with the ones obtained in Ref. [35] in the hard-wall model in the flavor symmetric case, where, depending on the different description of the scalar sector and chiral symmetry breaking, the contribution from the whole tower of axial-vector mesons lies in the range $39.9(17.2 + 22.7) - 43.3(18.3 + 25.0) \times 10^{-11}$. In Ref. [39] different masses for up/down and strange quarks have been considered and a Witten-Veneziano mass has been included, finding that the sum over the sectors for the whole meson tower is in the range $(30.5 - 33.7) \times 10^{-11}$ depending on how the parameters are set.

Let us conclude this section with a comment on the SDCs. The longitudinal component of the HLbL four-point function can be expressed as

TABLE II. Mass of the excited axial-vector mesons in the soft-wall model ($n = 0$ corresponds to the ground state), and their contribution to $a_\mu^{HLbL} (\times 10^{11})$. The value of a_μ^{HLbL} in the last column is the contribution from the whole tower of axial-vector mesons computed by the Green's function. In the last row we have emphasized the transverse (T) and longitudinal (L) contributions to $a_\mu^{HLbL} (\times 10^{11})$.

	$n = 0$	$n = 1$	$n = 2$	$n = 3$	$n = 4$	\sum_n
Mass (GeV)	1.7	2.7	3.5	4.2	4.9	
a_μ^{HLbL}	36	-0.5	3.7	-0.2	1.3	41.3
(T + L)	(16 + 20)	(-0.4 - 0.1)	(1.8 + 1.9)	(-0.13 - 0.07)	(0.65 + 0.67)	(18.1 + 23.2)

$$\Pi_{\mu\nu\alpha\beta}^{\parallel}(q_1, q_2, q_3, q_4) = T_{\mu\nu\alpha\beta}^{(1)}\bar{\Pi}_1 + T_{\mu\nu\alpha\beta}^{(2)}\bar{\Pi}_2 + T_{\mu\nu\alpha\beta}^{(3)}\bar{\Pi}_3 \quad (23)$$

with $T_{\mu\nu\alpha\beta}^{(1)} = \varepsilon_{\mu\nu\rho\sigma}\varepsilon_{\alpha\beta\rho'\sigma'}q_1^\rho q_2^\sigma q_3^{\rho'} q_4^{\sigma'}$, and $T^{(2,3)}$ and $\bar{\Pi}_{2,3}$ obtained by crossing operations [19]. The SDC conditions are [14]:

$$\lim_{Q_3 \rightarrow \infty} \lim_{Q \rightarrow \infty} Q^2 Q_3^2 \bar{\Pi}_1(Q, Q, Q_3) = -\frac{2}{3\pi^2} \quad (24)$$

$$\lim_{Q \rightarrow \infty} Q^4 \bar{\Pi}_1(Q, Q, Q) = -\frac{4}{9\pi^2}. \quad (25)$$

They have been checked in the hard-wall model in Ref. [20,35] and they are also obtained in the soft-wall model and agree with the considerations of Ref. [15]. The factorized contribution from pions scales as $1/Q^6$, of higher order in the $Q^2 \rightarrow \infty$ expansion than the result from the OPE. The longitudinal contribution from axial-vector mesons (obtained from the projector $\frac{q_\mu q_\nu M_A^2 - q^2}{q^2 M_A^2}$) is instead of the same order as the OPE result: it matches the OPE result in the region $Q_1^2 \sim Q_2^2 \gg Q_3^2 \gg m_\rho^2$, while in the region $Q_1^2 = Q_2^2 = Q_3^2 \gg m_\rho^2$ the correct power behavior is reproduced although the numerical factor is, both in the hard-wall and soft-wall models, 81% of the value in (25):

$$\lim_{Q \rightarrow \infty} Q^4 \bar{\Pi}_1(Q, Q, Q) \sim -\frac{0.36}{\pi^2}. \quad (26)$$

IV. TENSOR MESON CONTRIBUTION TO a_μ^{HLbL}

Tensor mesons with $J^{PC} = 2^{++}$ can be described in holographic models by a field dual to the $j_{\mu\nu} = \bar{q} \frac{1}{2} (\gamma_\mu i \overleftrightarrow{D}_\nu + \gamma_\nu i \overleftrightarrow{D}_\mu) q$ operator, i.e., by a symmetric tensor. In [41,42] the spin-2 field $h_{\mu\nu}$ (graviton) has been introduced as the $4d$ fluctuation of the metric (1):

$$ds^2 = g_{MN} dx^M dx^N = \frac{1}{z^2} (\eta_{\mu\nu} + h_{\mu\nu}) dx^\mu dx^\nu - \frac{1}{z^2} dz^2. \quad (27)$$

The action for $h_{\mu\nu}$ is obtained from the Einstein-Hilbert action:

$$S_{\text{EH}} = -2k_T \int d^5x \sqrt{g} (\mathcal{R} + 2\Lambda), \quad (28)$$

where \mathcal{R} is the Ricci scalar and Λ the cosmological constant. In the soft-wall model, in the quadratic approximation the action for the transverse traceless field $h_{\mu\nu}$ is (see the Appendix A):

$$S = -\frac{k_T}{2} \int d^5x \frac{e^{-\phi}}{z^3} \eta^{\mu\alpha} \eta^{\nu\beta} (\partial_z h_{\mu\nu} \partial_z h_{\alpha\beta} + h_{\mu\nu} \square h_{\alpha\beta}). \quad (29)$$

The coefficient k_T is fixed from the two-point correlation function. The field $h_{\mu\nu}$ has helicity ± 2 , and is a flavor singlet (representing singlet tensor mesons).

Higher spin mesons have been studied in [18,43–47] in holographic models, and a review on the description of fields with arbitrary spin in light-front holographic QCD can be found in [48]. In [18] a rank-2 symmetric tensor field H_{AB} is introduced, and, in the axial gauge $H_{Az} = 0$, the field $h_{\mu\nu}$, defined from $H_{\mu\nu} = h_{\mu\nu}/z^2$, obeys the same action (29).

From the action (29), the equation of motion in the Fourier space is

$$\partial_z \left(\frac{e^{-\phi}}{z^3} \partial_z h_{\mu\nu} \right) + \frac{e^{-\phi}}{z^3} q^2 h_{\mu\nu} = 0. \quad (30)$$

The two-point correlation function is found from the on-shell action:

$$S_{os} = \lim_{z \rightarrow 0} \frac{k_T}{2} \int d^4x \frac{e^{-\phi}}{z^3} \eta^{\mu\alpha} \eta^{\nu\beta} h_{\mu\nu} \partial_z h_{\alpha\beta} \quad (31)$$

deriving it with respect to the sources of the $4D$ tensor operator [49]. In the Fourier space the field $h_{\mu\nu}$ is related to the source $\hat{h}_{\mu\nu}$ by: $h_{\mu\nu}(z, q^2) = h_B(z, q^2) \hat{h}_{\mu\nu}(q^2)$, where h_B is the bulk-to-boundary propagator

$$h_B(z, q^2) = \Gamma \left(2 - \frac{q^2}{4c^2} \right) U \left(-\frac{q^2}{4c^2}, -1, c^2 z^2 \right) \quad (32)$$

obtained solving the equation of motion (30) with boundary conditions $h_B(0, q^2) = 1$ and finiteness of the action. The two-point function reads

$$\Pi^{\mu\nu\rho\sigma} = \frac{\delta^2 S_{os}}{\delta \hat{h}_{\mu\nu} \delta \hat{h}_{\rho\sigma}} = k_T P^{\mu\nu\rho\sigma} \lim_{z \rightarrow 0} \frac{e^{-\phi}}{z^3} h_B \partial_z h_B, \quad (33)$$

where $P_{\mu\nu\rho\sigma} = \frac{1}{2} (\eta_{\mu\rho} \eta_{\nu\sigma} + \eta_{\mu\sigma} \eta_{\nu\rho} - \frac{2}{3} \eta_{\mu\nu} \eta_{\rho\sigma})$ is the transverse projector. For $Q^2 = -q^2 \rightarrow \infty$ one has (ν is an energy scale)

$$\Pi^{\mu\nu\rho\sigma} \rightarrow -k_T P^{\mu\nu\rho\sigma} \frac{Q^4}{8} \log(Q^2/\nu^2) \quad (34)$$

to be compared with [41,50]

$$\Pi_{\text{QCD}}^{\mu\nu\rho\sigma} \rightarrow -P^{\mu\nu\rho\sigma} \left(\frac{N_c N_f}{160\pi^2} + \frac{N_c^2 - 1}{80\pi^2} \right) Q^4 \log(Q^2/\nu^2). \quad (35)$$

This condition fixes $k_T = \left(\frac{N_c N_f}{20\pi^2} + \frac{N_c^2 - 1}{10\pi^2} \right)$.

Eigenvalues and eigenfunctions are found by solving Eq. (30) requiring $h_n(0) = 0$ and normalization

$$\int_0^\infty dz \frac{e^{-\phi(z)}}{z^3} h_n(z)^2 = 1. \quad (36)$$

The spectrum is $m_n^2 = 4c^2(n+2)$ and the wave functions are [42]

$$h_n(z) = \sqrt{\frac{2}{(n+1)(n+2)}} c^3 z^4 L_n^2(c^2 z^2), \quad (37)$$

in terms of the generalized Laguerre polynomials $L_n^\lambda(z)$. The residues of the poles of the two-point function are $R_n = k_T 8c^6(n+1)(n+2)$. From $R_n = f_n^2 m_n^4$ we find the decay constants $f_n = c \sqrt{k_T(n+1)/(2(n+2))}$. For $c = 0.388$ GeV we obtain $m_{f_2} = 1.097$ GeV and $f_{f_2} = 69$ MeV (corresponding to $n = 0$), while the first excitation ($n = 1$) has mass $m_1 = 1.344$ GeV and decay constant $f_1 = 80$ MeV. The decay constant $g_f = f_{f_2}/m_{f_2} = \sqrt{5/2}/(8\pi) = 0.063$ can be compared to Ref. [51] where $g_f = 0.040$ is found, while in the hard-wall model one has $g_f = 0.024$ [41].

The decay $f_2 \rightarrow \gamma^* \gamma^*$ can be studied from the quadratic action of the electromagnetic field considering the fluctuation of the metric:

$$S_{f_2 \gamma \gamma} \supset -A_{f_2} \int d^5 x \sqrt{g} e^{-\phi} \text{Tr}(F_{MN} F^{MN}) \quad (38)$$

with $F_{MN} = \partial_M V_N - \partial_N V_M$ and $A_{f_2} = 1/4$. The obtained interaction is of the kind: $1/2 h_{\mu\nu} T^{\mu\nu}$, where $T^{\mu\nu}$ is the electromagnetic stress-energy tensor.

In the Fourier space, after introducing the source $V_\alpha(q)$ and the BTBP $V(z, q)$ (17) of the vector field, we find:

$$\begin{aligned} S_{f_2 \gamma \gamma} &= 2A_{f_2} \text{Tr}(Q_{em}^2 T^a) \int d^4 q_1 \int d^4 q_2 \\ &\times \int \frac{dz}{z} e^{-\phi} h_{\alpha\beta}^a(z, q_1 + q_2) V_\mu(q_1) V_\nu(q_2) \\ &\times (-\eta^{\mu\alpha} \eta^{\nu\beta} \partial_z V(z, q_1) \partial_z V(z, q_2) \\ &+ (q_1 \cdot q_2 \eta^{\mu\alpha} \eta^{\nu\beta} - q_1^\alpha q_2^\mu \eta^{\nu\beta} + q_1^\alpha q_2^\beta \eta^{\mu\nu} \\ &- q_1^\nu q_2^\beta \eta^{\mu\alpha}) V(z, q_1) V(z, q_2)). \end{aligned} \quad (39)$$

For a singlet field $T^a = T^0$. To find the amplitude, we derive the action with respect to the three sources of the fields, and write the BTBP of the tensor field as the sum

$$h(z, q^2) = \sum_n \frac{h_n(z) \sqrt{R_n/k_T}}{-q^2 + m_n^2}. \quad (40)$$

Identifying one transition form factor, the amplitude for $f_2 \rightarrow \gamma^* \gamma^*$ is

$$\begin{aligned} \mathcal{M}_{\mu\nu\alpha\beta} &= 4A_{f_2} \text{Tr}(Q_{em}^2 T^a) (q_1 \cdot q_2 \eta_{\mu\alpha} \eta_{\nu\beta} - q_{1\alpha} q_{2\mu} \eta_{\nu\beta} \\ &+ q_{1\alpha} q_{2\beta} \eta_{\mu\nu} - q_{1\nu} q_{2\beta} \eta_{\mu\alpha}) \int_0^\infty \frac{dz}{z} e^{-\phi} h_0(z) \\ &\times \left(-\frac{1}{q_1 \cdot q_2} \partial_z V(z, q_1) \partial_z V(z, q_2) \right. \\ &\left. + V(z, q_1) V(z, q_2) \right), \end{aligned} \quad (41)$$

where $h_0(z)$ is the wave function of the ground state, obtained from (37) for $n = 0$. The amplitude in (41) has the same Lorentz structure given in [52]. In [30] a different form of the amplitude has been proposed. From Eq. (41) the two-photon transition form factor can be extracted ($q_i^2 = -Q_i^2$):

$$\begin{aligned} F_{f_2 \gamma^* \gamma^*}(Q_1^2, Q_2^2) &= \frac{4}{\sqrt{k_T}} A_{f_2} \text{Tr}(Q_{em}^2 T^a) \int_0^\infty \frac{dz}{z} e^{-\phi} h_0^a(z) \\ &\times \left(\frac{-2}{m_0^2 + Q_1^2 + Q_2^2} \partial_z V(z, Q_1^2) \partial_z V(z, Q_2^2) \right. \\ &\left. + V(z, Q_1^2) V(z, Q_2^2) \right). \end{aligned} \quad (42)$$

Equation (42) can also be used to compute the TFF in the hard-wall model with some modifications: the upper limit of the integral is $z_0 = (322 \text{ MeV})^{-1}$, the dilaton vanishes, the tensor wave function is [41]

$$h_0^{HW}(z) = 3.51 \frac{z^2}{z_0} J_2(m_0 z) \quad (43)$$

with the tensor mass $m_0 = 1.23$ GeV, the vector BTBP is [20]

$$\begin{aligned} V^{HW}(z, Q^2) &= \sqrt{Q^2} z \left(K_1(\sqrt{Q^2} z) \right. \\ &\left. + I_1(\sqrt{Q^2} z) \frac{K_0(\sqrt{Q^2} z_0)}{I_0(\sqrt{Q^2} z_0)} \right). \end{aligned} \quad (44)$$

If one photon is real, only the second term in (42) contributes to $F_{f_2 \gamma^* \gamma}$, and its behavior in the soft-wall and hard-wall models is shown in Fig. 3 together with data for the helicity-2 component of $f_2(1270)$ from Belle collaboration [53]. The curve obtained in the hard-wall model has a better agreement with the experimental points, and this is due to the fact that the ground-state mass prediction of the HW is closer to the experimental $f_2(1270)$ mass than the SW prediction. Indeed, if the $f_2(1270)$ mass is used to fix the mass scale c in the soft-wall model, the TFF in the SW and HW models are similar. In Fig. 4 the results from [54] and two determinations from [32] are also shown. In Fig. 5 $F_{f_2 \gamma^* \gamma^*}(Q^2, Q^2)$ for two photons with equal virtualities is shown. The $f_2(1270) \rightarrow \gamma \gamma$ decay width is $\Gamma_{\gamma\gamma} = 2.6 \pm 0.5$ keV [55], and it is related to the form factor by

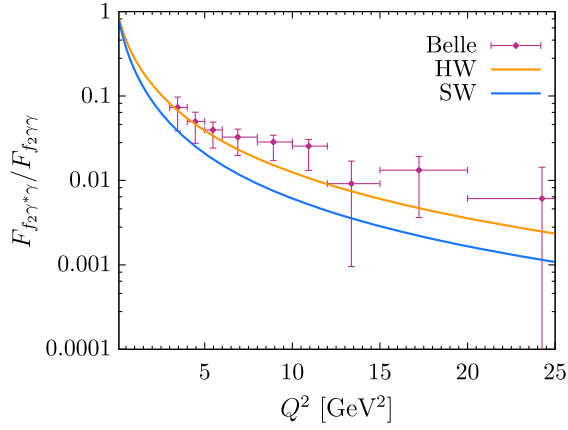


FIG. 3. f_2 TFF with one real and one virtual photon in the soft-wall (blue curve) and hard-wall (orange curve) models. Belle data are from Ref. [53].

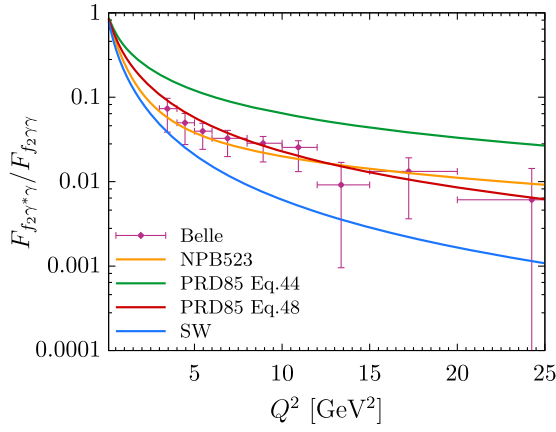


FIG. 4. f_2 TFF with one real and one virtual photon in the soft-wall model (blue curve), compared with results found in other models: Ref. [54] (orange curve), [32] (green and red curves). Belle data are from Ref. [53].

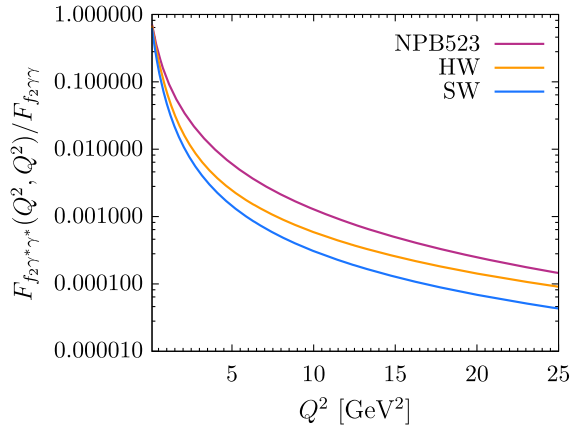


FIG. 5. f_2 TFF with two virtual photons in the soft-wall model (blue curve), hard-wall (orange curve) model and computed in Ref. [54] (magenta curve).

$$\Gamma_{\gamma\gamma} = \frac{\pi\alpha^2}{20} m_0^3 F_{f_2\gamma\gamma}^2, \quad (45)$$

which fixes $F_{f_2\gamma\gamma} = 0.387 \text{ GeV}^{-1}$. From Eq. (42), the form factor for two real photons is $F_{f_2\gamma\gamma} = 4A_{f_2}/\sqrt{k_T}\text{Tr}(Q_{em}^2 T^0)/2c$ in the soft-wall model. Using $A_{f_2} = 1/4$ we find $F_{f_2\gamma\gamma} = 0.986 \text{ GeV}^{-1}$. In the hard-wall model one has $F_{f_2\gamma\gamma} = 4A_{f_2}/\sqrt{k_T}\text{Tr}(Q_{em}^2 T^0)(2.084 \text{ GeV}^{-1})$, hence $A_{f_2} = 1/4$ produces $F_{f_2\gamma\gamma} = 1.594 \text{ GeV}^{-1}$.

The results can be extended to non-singlet tensor mesons. As previously noticed, the action (29) is used to describe also a generic tensor field dual to the operator

$j_{\mu\nu} = \bar{q}\frac{1}{2}(\gamma_\mu i\vec{D}_\nu + \gamma_\nu i\vec{D}_\mu)q$, without considering the fluctuations of the metric. Assuming its coupling to two photons is described by the action (39), we consider the product $\tilde{A}_{f_2} = A_{f_2}\text{Tr}(Q_{em}^2 T^a)$ as a free parameter and we fix it from $F_{f_2\gamma\gamma} = 0.387 \text{ GeV}^{-1}$. We get $\tilde{A}_{f_2} = 0.0267$ in the soft-wall model and $\tilde{A}_{f_2} = 0.0165$ in the hard-wall model. We shall use such values of \tilde{A}_{f_2} to compute the contribution to a_μ from $f_2(1270)$.

As done for axial-vector mesons, the asymptotic large- Q^2 behavior of the f_2 TFF can be analytically obtained from Eq. (42) defining the variables $Q^2 = (Q_1^2 + Q_2^2)/2$ and $w = (Q_1^2 - Q_2^2)/(Q_1^2 + Q_2^2)$, noticing that in the soft-wall model $V(z, Q^2) \xrightarrow{Q^2 \rightarrow \infty} z\sqrt{Q^2}K_1(z\sqrt{Q^2})$ [27] and $h_0(z) = f_0 m_0^2/(4\sqrt{k_T})z^4$. We find:

$$\begin{aligned} F_{f_2\gamma^*\gamma^*} \xrightarrow{Q^2 \rightarrow \infty} & F_{f_2\gamma\gamma} 2c \frac{f_0 m_0^2}{4\sqrt{k_T} Q^4} \int_0^\infty dx x^5 \\ & \times \left[-(1-w^2)K_0(x\sqrt{1+w})K_0(x\sqrt{1-w}) \right. \\ & \left. + \sqrt{1-w^2}K_1(x\sqrt{1+w})K_1(x\sqrt{1-w}) \right] \\ & = \frac{F_{f_2\gamma\gamma}}{4\sqrt{2k_T}} \frac{f_0 m_0^3}{Q^4 w^5} \left(4w(6-5w^2) + 2(6-7w^2+w^4) \right. \\ & \left. \times \log \frac{1-w}{1+w} \right). \end{aligned} \quad (46)$$

In [36] this expansion has been computed in perturbative QCD. The form factor multiplying the tensor

$$T_1^{\mu\nu\alpha\beta} = 2q_1 \cdot q_2 \eta^{\mu\alpha} \eta^{\nu\beta} - 2q_1^\alpha q_2^\mu \eta^{\nu\beta} + 2q_1^\alpha q_2^\beta \eta^{\mu\nu} - 2q_1^\nu q_2^\beta \eta^{\mu\alpha} \quad (47)$$

at large Q^2 is

$$\mathcal{F}_1^T(q_1^2, q_2^2) = \frac{4\sum_a C_a F_A^a m_T^3}{Q^4} f_1^T(w) \quad (48)$$

with

$$f_1^T(w) = \frac{5(1-w^2)}{8w^6} \left(15 - 4w^2 + \frac{3(5-3w^2)}{2w} \log \frac{1-w}{1+w} \right) \quad (49)$$

having the same Q^2 but a different w behavior than in Eq. (46).

The results for the TFF can be used to compute the HLbL pole contribution of tensor mesons to muon $g-2$ using Eq. (B9) in Appendix B. We find that the $f_2(1270)$ contribution to muon $g-2$ is $a_\mu^{HLbL} \sim 0.61 \times 10^{-11}$ in the soft-wall model and $a_\mu^{HLbL} \sim 0.63 \times 10^{-11}$ in the hard-wall model. They agree with the result in [30] $a_\mu^{HLbL} = (0.79 \pm 0.09) \times 10^{-11}$. In Ref. [56] $a_\mu^{HLbL} = (0.50 \pm 0.13) \times 10^{-11}$ and $a_\mu^{HLbL} = (0.21 \pm 0.05) \times 10^{-11}$ are obtained for $f_2(1270)$ and $f_2(1565)$, respectively.

V. CONCLUSIONS

Holographic bottom-up models, despite their simplicity, provide a good qualitative description of QCD observables in different sectors, and in some case succeed in quantitative predictions. This also holds for the two-photon transition form factors of axial-vector and tensor mesons. The TFF of tensor mesons in the soft-wall model is smaller than experimental values but the differences are within the experimental errors. A better agreement is found between the hard-wall model and experimental data, since the mass prediction better reproduces the measured $f_2(1270)$ mass. The results for axial-vector and tensor meson contributions to the anomalous magnetic moment of the muon confirm the decreasing hierarchy from pseudoscalar, axial-vector and tensor meson poles. The values we have found in the soft-wall model are $a_\mu^{HLbL} = 36 \times 10^{-11}$ for axial-vector mesons and $a_\mu^{HLbL} = 0.61 \times 10^{-11}$ for tensor mesons. The contribution from the pion computed in [28] in a model that for pions is identical to the one considered in this paper is $a_\mu^{HLbL} = 75.2 \times 10^{-11}$ for the ground state and $a_\mu^{HLbL} = 1.68 \times 10^{-11}$ for the first excited state. It would be interesting to extend the present analysis considering the model of Ref. [28] with the strange quark mass and the $U(1)_A$ anomaly. This is left to a future study.

ACKNOWLEDGMENTS

We thank Luigi Cappiello, Josef Leutgeb, Jonas Mager, Pere Masjuan, Anton Rebhan, Pablo Roig and Pablo Sanchez-Puertas for discussions. The work is carried out within the INFN project (Iniziativa Specifica) SPIF. It has been partly funded by the European Union—Next Generation EU through the research Grant No. P2022Z4P4B “SOPHYA—Sustainable Optimised PHYSics Algorithms: fundamental physics to build an advanced society” under the program PRIN 2022 PNRR of the Italian Ministero dell’Università e Ricerca (MUR).

APPENDIX A: TENSOR MESON ACTION

Let us compute the Einstein-Hilbert action for the metric

$$ds^2 = g_{MN} dx^M dx^N = \frac{1}{z^2} (\eta_{\mu\nu} + \lambda h_{\mu\nu}) dx^\mu dx^\nu - \frac{1}{z^2} dz^2, \quad (A1)$$

where $h_{\mu\nu}$ is a small fluctuation of the metric and λ a parameter. We consider a transverse symmetric tensor, hence $\partial^\mu h_{\mu\nu} = 0$ and $h_{\mu\nu} = h_{\nu\mu}$. The Einstein-Hilbert action is

$$S_{\text{EH}} = -2k_T \int d^5x \sqrt{g} (\mathcal{R} + 2\Lambda), \quad (A2)$$

where \mathcal{R} is the Ricci scalar and Λ the cosmological constant. At $\mathcal{O}(\lambda^0)$ the metric describes a 5D AdS space, with $\mathcal{R}^{(0)} = 20$ and $\Lambda = -6$. To $\mathcal{O}(\lambda^2)$ we find:

$$g^{\mu\nu} = z^2 (\eta^{\mu\nu} - \lambda h^{\mu\nu} + \lambda^2 h^{\mu\alpha} h_\alpha^\nu) + \mathcal{O}(\lambda^3) \quad (A3)$$

$$\sqrt{g} = z^{-5} \left(1 + \frac{\lambda}{2} h + \lambda^2 \left(-\frac{1}{4} h^{\mu\nu} h_{\mu\nu} + \frac{1}{8} h^2 \right) \right) + \mathcal{O}(\lambda^3), \quad (A4)$$

where $h^{\mu\nu} = \eta^{\alpha\mu} \eta^{\beta\nu} h_{\alpha\beta}$ and $h = \eta^{\mu\nu} h_{\mu\nu}$,

$$R_{zz} = -\frac{4}{z^2} + \lambda \left(\frac{1}{2z} \partial_z h - \frac{1}{2} \partial_z^2 h \right) + \lambda^2 \left(\frac{1}{2} \partial_z (h^{\alpha\beta} \partial_z h_{\alpha\beta}) - \frac{1}{4} (\partial_z h^{\alpha\beta}) (\partial_z h_{\alpha\beta}) - \frac{1}{2z} h^{\alpha\beta} \partial_z h_{\alpha\beta} \right) + \mathcal{O}(\lambda^3) \quad (A5)$$

$$\begin{aligned} R_{\mu\nu} = & \frac{4}{z^2} \eta_{\mu\nu} + \lambda \left(\frac{4}{z^2} h_{\mu\nu} - \frac{3}{2z} \partial_z h_{\mu\nu} + \frac{1}{2} \partial_z^2 h_{\mu\nu} - \frac{1}{2} \square h_{\mu\nu} - \frac{1}{2} \partial_\mu \partial_\nu h - \frac{1}{2z} \eta_{\mu\nu} \partial_z h \right) \\ & + \lambda^2 \left(-\frac{1}{2z} h_{\mu\nu} \partial_z h + \frac{1}{4} (\partial_z h) (\partial_z h_{\mu\nu}) + \frac{1}{2z} \eta_{\mu\nu} h^{\alpha\beta} \partial_z h_{\alpha\beta} - \frac{1}{4} (\partial_\beta h) \partial^\beta h_{\mu\nu} \right. \\ & \left. - \frac{1}{2} (\partial_z h_{\mu\beta}) \partial_z h_\nu^\beta - \frac{1}{4} (\partial_\mu h^{\alpha\beta}) \partial_\nu h_{\alpha\beta} + \frac{1}{2} (\partial_\beta h_\mu^\alpha) \partial^\beta h_{\nu\alpha} \right) + \mathcal{O}(\lambda^3). \end{aligned} \quad (A6)$$

In \mathcal{R} the $h_{\mu\nu}$ and h decouple. Since we are interested in a spin-2 field, we do not consider terms depending on h :

$$\begin{aligned} \mathcal{R} = & 20 + \lambda^2 \left(4z h^{\alpha\beta} \partial_z h_{\alpha\beta} - \frac{z^2}{4} (\partial_z h^{\alpha\beta})(\partial_z h_{\alpha\beta}) + \frac{z^2}{4} (\partial_\mu h^{\alpha\beta})(\partial^\mu h_{\alpha\beta}) - \frac{z^2}{2} h^{\alpha\beta} \partial_z^2 h_{\alpha\beta} \right. \\ & \left. + \frac{z^2}{2} h^{\alpha\beta} \square h_{\alpha\beta} - \frac{z^2}{2} \partial_z (h^{\alpha\beta} \partial_z h_{\alpha\beta}) \right) + \mathcal{O}(\lambda^3). \end{aligned} \quad (\text{A7})$$

Finally, we expand the Lagrangian:

$$\begin{aligned} \sqrt{g}(\mathcal{R} + 2\Lambda) = & \frac{8}{z^5} + \lambda^2 \left(\frac{4}{z^4} h^{\alpha\beta} \partial_z h_{\alpha\beta} - \frac{1}{4z^3} (\partial_z h^{\alpha\beta})(\partial_z h_{\alpha\beta}) + \frac{1}{4z^3} (\partial_\mu h^{\alpha\beta})(\partial^\mu h_{\alpha\beta}) \right. \\ & \left. - \frac{1}{2z^3} h^{\alpha\beta} \partial_z^2 h_{\alpha\beta} + \frac{1}{2z^3} h^{\alpha\beta} \square h_{\alpha\beta} - \frac{1}{2z^3} \partial_z (h^{\alpha\beta} \partial_z h_{\alpha\beta}) - \frac{2}{z^5} h^{\alpha\beta} h_{\alpha\beta} \right) + \mathcal{O}(\lambda^3) \\ = & \frac{8}{z^5} + \lambda^2 \left(\partial_z \left(\frac{1}{2z^4} h^{\alpha\beta} h_{\alpha\beta} \right) + \frac{1}{4z^3} (\partial_z h^{\alpha\beta})(\partial_z h_{\alpha\beta}) + \frac{1}{4z^3} h^{\alpha\beta} \square h_{\alpha\beta} \right. \\ & \left. - \partial_z \left(\frac{1}{z^3} h^{\alpha\beta} \partial_z h_{\alpha\beta} \right) \right) + \mathcal{O}(\lambda^3). \end{aligned} \quad (\text{A8})$$

The Gibbons-Hawking-York boundary term is:

$$S_{GHY} = -4k_T \int_{\partial} d^4x \sqrt{\gamma} K, \quad (\text{A9})$$

where γ is the determinant of the induced metric on the boundary ∂ of the spacetime and K the extrinsic curvature. At $\mathcal{O}(\lambda^2)$ it reads:

$$S_{GHY}^{(2)} = -2k_T \int_{\partial} d^4x \left(-\frac{2}{z^4} h^{\mu\nu} h_{\mu\nu} + \frac{1}{z^3} h^{\mu\nu} \partial_z h_{\mu\nu} \right). \quad (\text{A10})$$

The total action at $\mathcal{O}(\lambda^2)$ is then:

$$\begin{aligned} S^{(2)} = & -2k_T \int d^5x \left(\frac{1}{4z^3} (\partial_z h^{\alpha\beta})(\partial_z h_{\alpha\beta}) + \frac{1}{4z^3} h^{\alpha\beta} \square h_{\alpha\beta} \right) \\ & + 3k_T \int_{\partial} d^4x \frac{1}{z^4} h^{\mu\nu} h_{\mu\nu}. \end{aligned} \quad (\text{A11})$$

Neglecting the last (boundary) term, the action considered in the soft-wall model in Sec. IV is

$$S = -\frac{k_T}{2} \int d^5x e^{-\phi} \left(\frac{1}{z^3} (\partial_z h^{\alpha\beta})(\partial_z h_{\alpha\beta}) + \frac{1}{z^3} h^{\alpha\beta} \square h_{\alpha\beta} \right). \quad (\text{A12})$$

APPENDIX B: a_{μ}^{HLbL} FROM TENSOR MESON POLES

The HLbL contribution to the anomalous magnetic moment of the muon is computed from [3]:

$$\begin{aligned} a_{\mu}^{HLbL} = & -\frac{ie^6}{48m_{\mu}} \int \frac{d^4q_1}{(2\pi)^4} \int \frac{d^4q_2}{(2\pi)^4} \frac{1}{q_1^2 q_2^2 (k - q_1 - q_2)^2} \\ & \times \frac{1}{(p - q_1)^2 - m_{\mu}^2} \frac{1}{(p - q_1 - q_2)^2 - m_{\mu}^2} \\ & \times \text{Tr}((\not{p} + m_{\mu})[\gamma^{\rho}, \gamma^{\sigma}](\not{p} + m_{\mu})\gamma^{\mu} \\ & \times (\not{p} - \not{q}_1 + m_{\mu})\gamma^{\nu}(\not{p} - \not{q}_1 - \not{q}_2 + m_{\mu})\gamma^{\lambda}) \\ & \times \frac{\partial}{\partial k^{\rho}} \Pi_{\mu\nu\lambda\sigma}(q_1, q_2, k - q_1 - q_2) \Big|_{k \rightarrow 0}, \end{aligned} \quad (\text{B1})$$

where p denotes the initial muon momentum, m_{μ} is the muon mass, q_1, q_2, q_3, q_4 are the momenta of the incoming photons, and $k = -q_4$. Let us consider the contribution to $\Pi_{\mu\nu\lambda\sigma}$ from tensor-meson exchange [30]:

$$\begin{aligned} & (ie)^4 \Pi_{\mu\nu\lambda\sigma}^T(q_1, q_2, q_3) \\ & = \mathcal{M}_{\mu\nu\alpha\alpha'}(q_1, q_2) \frac{iP^{\alpha\alpha'\beta\beta'}(k - q_3)}{(k - q_3)^2 - M_T^2} \mathcal{M}_{\lambda\sigma\beta\beta'}(q_3, -k) \\ & + \mathcal{M}_{\mu\sigma\alpha\alpha'}(q_1, -k) \frac{iP^{\alpha\alpha'\beta\beta'}(k - q_1)}{(k - q_1)^2 - M_T^2} \mathcal{M}_{\nu\lambda\beta\beta'}(q_2, q_3) \\ & + \mathcal{M}_{\mu\lambda\alpha\alpha'}(q_1, q_3) \frac{iP^{\alpha\alpha'\beta\beta'}(k - q_2)}{(k - q_2)^2 - M_T^2} \mathcal{M}_{\nu\sigma\beta\beta'}(q_2, -k) \end{aligned} \quad (\text{B2})$$

with M_T the mass of the tensor meson. We only consider the dominant contribution from helicity $\Lambda = 2$ [30], for which the amplitude of the f_2 production from two photons is written as [52]

$$\begin{aligned} \mathcal{M}^{\mu\nu\alpha\beta}(q_1, q_2) = & e^2 (q_1 \cdot q_2 \eta^{\mu\alpha} \eta^{\nu\beta} - q_1^{\alpha} q_2^{\mu} \eta^{\nu\beta} + q_1^{\alpha} q_2^{\beta} \eta^{\mu\nu} \\ & - q_1^{\nu} q_2^{\beta} \eta^{\mu\alpha}) F_{T\gamma^* \gamma^*}(q_1^2, q_2^2), \end{aligned} \quad (\text{B3})$$

where α, β are f_2 indices. The projection operator for $J = 2$ has the form:

$$P_{\alpha\beta\gamma\delta}(p) = \frac{1}{2}((-g_{\alpha\gamma} + p_\alpha p_\gamma/p^2)(-g_{\beta\delta} + p_\beta p_\delta/p^2) + (-g_{\alpha\delta} + p_\alpha p_\delta/p^2)(-g_{\beta\gamma} + p_\beta p_\gamma/p^2)) - \frac{1}{3}(-g_{\alpha\beta} + p_\alpha p_\beta/p^2)(-g_{\gamma\delta} + p_\gamma p_\delta/p^2). \quad (\text{B4})$$

We define the momenta $Q_i = iq_i$ and $P = ip$, obtaining:

$$a_\mu^{\text{HLbL}} = \frac{e^6}{48m_\mu} \int \frac{d^4 Q_1}{(2\pi)^4} \int \frac{d^4 Q_2}{(2\pi)^4} \frac{1}{Q_1^2 Q_2^2 (Q_1 + Q_2)^2} \frac{1}{(P + Q_1)^2 + m_\mu^2} \frac{1}{(P - Q_2)^2 + m_\mu^2} \times \left(T_1(Q_1, Q_2, P) \frac{F_{T\gamma^*\gamma^*}(Q_1^2, (Q_1 + Q_2)^2) F_{T\gamma^*\gamma^*}(Q_2^2, 0)}{Q_2^2 + M_T^2} + T_2(Q_1, Q_2, P) \frac{F_{T\gamma^*\gamma^*}((Q_1 + Q_2)^2, Q_2^2) F_{T\gamma^*\gamma^*}(Q_1^2, 0)}{Q_1^2 + M_T^2} + T_3(Q_1, Q_2, P) \frac{F_{T\gamma^*\gamma^*}(Q_1^2, Q_2^2) F_{T\gamma^*\gamma^*}((Q_1 + Q_2)^2, 0)}{(Q_1 + Q_2)^2 + M_T^2} \right), \quad (\text{B5})$$

with

$$T_1 = \frac{32m_\mu}{3Q_2^2} ((P \cdot Q_2)^2 (-6(Q_1 \cdot Q_2)^2 + 2Q_1^2 Q_2^2) + Q_2^2 ((8m_\mu^2 - 4P \cdot Q_1)(Q_1 \cdot Q_2)^2 + 2(-2(P \cdot Q_1)^2 + m_\mu^2 Q_1^2 + 2P \cdot Q_1 Q_1^2) Q_2^2 + 5(2m_\mu^2 - P \cdot Q_1) Q_1 \cdot Q_2 Q_2^2) + P \cdot Q_2 (4(Q_1 \cdot Q_2)^3 + 2(9P \cdot Q_1 - 2Q_1^2) Q_1 \cdot Q_2 Q_2^2 + 5(Q_1 \cdot Q_2)^2 Q_2^2 + 10P \cdot Q_1 Q_2^4)) \quad (\text{B6})$$

$$T_3 = -\frac{32m_\mu}{3(Q_1 + Q_2)^2} ((P \cdot Q_2)^2 (4Q_1^4 + 6(Q_1 \cdot Q_2)^2 + Q_1^2 (8Q_1 \cdot Q_2 - 2Q_2^2)) + (P \cdot Q_1)^2 (6(Q_1 \cdot Q_2)^2 + 8Q_1 \cdot Q_2 Q_2^2 - 2(Q_1^2 - 2Q_2^2) Q_2^2) - 3P \cdot Q_2 (Q_1^2 + Q_1 \cdot Q_2) (Q_1^2 (5Q_1 \cdot Q_2 + 2Q_2^2) + Q_1 \cdot Q_2 (8Q_1 \cdot Q_2 + 5Q_2^2)) + 2m_\mu^2 (Q_1^4 (5Q_1 \cdot Q_2 + 4Q_2^2) + 2Q_1^2 (8(Q_1 \cdot Q_2)^2 + 9Q_1 \cdot Q_2 Q_2^2 + 2Q_2^4) + Q_1 \cdot Q_2 (12(Q_1 \cdot Q_2)^2 + 16Q_1 \cdot Q_2 Q_2^2 + 5Q_2^4)) + P \cdot Q_1 (2P \cdot Q_2 (5Q_1^4 + 18(Q_1 \cdot Q_2)^2 + 16Q_1 \cdot Q_2 Q_2^2 + 5Q_2^4) + 4Q_1^2 (4Q_1 \cdot Q_2 + Q_2^2)) + 3(Q_1 \cdot Q_2 + Q_2^2) (Q_1^2 (5Q_1 \cdot Q_2 + 2Q_2^2) + Q_1 \cdot Q_2 (8Q_1 \cdot Q_2 + 5Q_2^2))). \quad (\text{B7})$$

The second term in (B5) coincides with the first one after changing variables $Q_1 \rightarrow -Q_2$ and $Q_2 \rightarrow -Q_1$. To eliminate the dependence on the direction of the muon momentum P , we average over all spatial directions of P

$$a_\mu^{\text{HLbL}} = \frac{1}{2\pi^2} \int d\Omega(\hat{P}) a_\mu^{\text{HLbL}}. \quad (\text{B8})$$

The integrals can be done analytically expressing the propagators in terms of Gegenbauer polynomials [3]. Defining $t = \cos\theta$, with θ the angle between the four vectors Q_1 and Q_2 , and $Q_1 = |Q_1|$ and $Q_2 = |Q_2|$, we obtain

$$a_\mu^{\text{HLbL}} = \frac{\alpha^3}{24\pi^2 m_\mu} \int_0^\infty dQ_1 \int_0^\infty dQ_2 \int_{-1}^1 dt \sqrt{1-t^2} \frac{Q_1 Q_2}{Q_3^2} \left(I_1(Q_1, Q_2, t) \frac{F_{T\gamma^*\gamma^*}(Q_1^2, Q_2^2) F_{T\gamma^*\gamma^*}(Q_2^2, 0)}{Q_2^2 + M_T^2} + \left(I_2(Q_1, Q_2, t) \frac{F_{T\gamma^*\gamma^*}(Q_1^2, Q_2^2) F_{T\gamma^*\gamma^*}(Q_3^2, 0)}{Q_3^2 + M_T^2} \right) \right), \quad (\text{B9})$$

with

$$\begin{aligned}
I_1(Q_1, Q_2, t) = & \frac{8Q_2}{3m_\mu} (-10Q_2^3 - 6Q_1Q_2^2t - 4m_\mu^2(5Q_2 + 9Q_1t) + 4Q_1^2Q_2(-5 + 3t^2) \\
& + Q_1^3t(-27 + 11t^2) - 2Q_1^2(2Q_2 + 7Q_1t)(-2 + t^2)R_1 + Q_1^3t(-1 + 3t^2)R_1^2 \\
& + 2Q_2R_2(5Q_2^2 + 2Q_1Q_2t + Q_1^2(6 - 4t^2) + Q_1Q_2tR_2) + 8Q_1Q_2(2m_\mu^2(Q_1 + 5Q_2t + 4Q_1t^2) \\
& + Q_1(Q_2^2(-2 + t^2) + 2Q_1Q_2t(-2 + t^2) + Q_1^2(-3 + 2t^2)))X(Q_1, Q_2, t))
\end{aligned} \tag{B10}$$

$$\begin{aligned}
I_2(Q_1, Q_2, t) = & \frac{4}{3m_\mu Q_3^2} (2(5Q_1^6 + 5Q_2^6 + 32Q_1^5Q_2t + 32Q_1Q_2^5t + Q_1^3Q_2^3t(65 + 51t^2) + Q_1^4Q_2^2(14 + 71t^2) \\
& + Q_1^2Q_2^4(14 + 71t^2) + 2m_\mu^2(5Q_1^4 + 5Q_2^4 + 16Q_1^3Q_2t + 16Q_1Q_2^3t + 2Q_1^2Q_2^2(2 + 9t^2))) \\
& - 2Q_1^2(5Q_1^4 + 33Q_1^3Q_2t + 6Q_2^4(1 + 2t^2) + Q_1Q_2^3t(32 + 27t^2) + Q_1^2Q_2^2(8 + 61t^2))R_1 \\
& + Q_1^3Q_2t(2Q_1^2 + 4Q_1Q_2t + Q_2^2(-1 + 3t^2))R_1^2 + Q_2(Q_2R_2(-2(5Q_2^4 + 33Q_1Q_2^3t + 6Q_1^4(1 + 2t^2) \\
& + Q_1^3Q_2t(32 + 27t^2) + Q_1^2Q_2^2(8 + 61t^2)) + Q_1Q_2t(2Q_2^2 + 4Q_1Q_2t + Q_1^2(-1 + 3t^2))R_2) \\
& + 8Q_1(Q_1^2 + Q_2^2 + 2Q_1Q_2t)(-2m_\mu^2(4Q_1Q_2 + 5(Q_1^2 + Q_2^2)t + 6Q_1Q_2t^2) \\
& + 3Q_1Q_2(Q_1^2 + Q_2^2 + 6Q_1Q_2t + 2(Q_1^2 + Q_2^2)t^2))X(Q_1, Q_2, t))
\end{aligned} \tag{B11}$$

and $Q_3^2 = Q_1^2 + 2Q_1Q_2t + Q_2^2$, $X(Q_1, Q_2, t) = \frac{1}{Q_1Q_2\sqrt{1-t^2}} \arctan\left(\frac{z\sqrt{1-t^2}}{1-zt}\right)$, $z = \frac{Q_1Q_2}{4m_\mu^2}(1 - R_1)(1 - R_2)$, $R_i = \sqrt{1 + 4m_\mu^2/Q_i^2}$.

-
- [1] D. P. Aguillard *et al.* (Muon g-2 Collaboration), Measurement of the positive muon anomalous magnetic moment to 0.20 ppm, *Phys. Rev. Lett.* **131**, 161802 (2023).
- [2] T. Aoyama *et al.*, The anomalous magnetic moment of the muon in the standard model, *Phys. Rep.* **887**, 1 (2020).
- [3] F. Jegerlehner and A. Nyffeler, The Muon g-2, *Phys. Rep.* **477**, 1 (2009).
- [4] G. Colangelo, M. Hoferichter, and P. Stoffer, Two-pion contribution to hadronic vacuum polarization, *J. High Energy Phys.* **02** (2019) 006.
- [5] G. Colangelo, M. Hoferichter, M. Procura, and P. Stoffer, Dispersion relation for hadronic light-by-light scattering: two-pion contributions, *J. High Energy Phys.* **04** (2017) 161.
- [6] D. Melo-Porrás, E. A. Reyes Rojas, and A. R. Fazio, Hadronic light by light corrections to the muon anomalous magnetic moment, *Particles* **7**, 327 (2024).
- [7] S. Borsanyi *et al.*, Leading hadronic contribution to the muon magnetic moment from lattice QCD, *Nature (London)* **593**, 51 (2021).
- [8] L. Di Luzio, A. Masiero, P. Paradisi, and M. Passera, New physics behind the new muon g-2 puzzle?, *Phys. Lett. B* **829**, 137037 (2022).
- [9] J. P. Lees *et al.* (BABAR Collaboration), Precise measurement of the $e^+e^- \rightarrow \pi^+\pi^-(\gamma)$ cross section with the initial-state radiation method at BABAR, *Phys. Rev. D* **86**, 032013 (2012).
- [10] A. Anastasi *et al.* (KLOE-2 Collaboration), Combination of KLOE $\sigma(e^+e^- \rightarrow \pi^+\pi^-\gamma(\gamma))$ measurements and determination of $a_\mu^{\pi^+\pi^-}$ in the energy range $0.10 < s < 0.95$ GeV², *J. High Energy Phys.* **03** (2018) 173.
- [11] F. V. Ignatov *et al.* (CMD-3 Collaboration), Measurement of the $e^+e^- \rightarrow \pi^+\pi^-$ cross section from threshold to 1.2 GeV with the CMD-3 detector, [arXiv:2302.08834](https://arxiv.org/abs/2302.08834).
- [12] A. Crivellin, M. Hoferichter, C. A. Manzari, and M. Montull, Hadronic vacuum polarization: $(g-2)_\mu$ versus global electroweak fits, *Phys. Rev. Lett.* **125**, 091801 (2020).
- [13] G. Colangelo *et al.*, Prospects for precise predictions of a_μ in the standard model, [arXiv:2203.15810](https://arxiv.org/abs/2203.15810).
- [14] K. Melnikov and A. Vainshtein, Hadronic light-by-light scattering contribution to the muon anomalous magnetic moment revisited, *Phys. Rev. D* **70**, 113006 (2004).
- [15] P. Masjuan, P. Roig, and P. Sanchez-Puertas, The interplay of transverse degrees of freedom and axial-vector mesons with short-distance constraints in g-2, *J. Phys. G* **49**, 015002 (2022).
- [16] G. Colangelo, F. Hagelstein, M. Hoferichter, L. Laub, and P. Stoffer, Short-distance constraints on hadronic light-by-light scattering in the anomalous magnetic moment of the muon, *Phys. Rev. D* **101**, 051501 (2020).
- [17] G. Colangelo, F. Hagelstein, M. Hoferichter, L. Laub, and P. Stoffer, Longitudinal short-distance constraints for the hadronic light-by-light contribution to $(g-2)_\mu$ with large- N_c Regge models, *J. High Energy Phys.* **03** (2020) 101.
- [18] A. Karch, E. Katz, D. T. Son, and M. A. Stephanov, Linear confinement and AdS/QCD, *Phys. Rev. D* **74**, 015005 (2006).

- [19] L. Cappiello, O. Catà, G. D'Ambrosio, D. Greynat, and A. Iyer, Axial-vector and pseudoscalar mesons in the hadronic light-by-light contribution to the muon ($g - 2$), *Phys. Rev. D* **102**, 016009 (2020).
- [20] J. Leutgeb and A. Rebhan, Axial vector transition form factors in holographic QCD and their contribution to the anomalous magnetic moment of the muon, *Phys. Rev. D* **101**, 114015 (2020).
- [21] P. Colangelo, F. De Fazio, F. Giannuzzi, F. Jugeau, and S. Nicotri, Light scalar mesons in the soft-wall model of AdS/QCD, *Phys. Rev. D* **78**, 055009 (2008).
- [22] P. Colangelo, F. De Fazio, F. Jugeau, and S. Nicotri, On the light glueball spectrum in a holographic description of QCD, *Phys. Lett. B* **652**, 73 (2007).
- [23] L. Bellantuono, P. Colangelo, and F. Giannuzzi, Holographic oddballs, *J. High Energy Phys.* **10** (2015) 137.
- [24] L. Bellantuono, P. Colangelo, and F. Giannuzzi, Exotic $J^{PC} = 1^{-+}$ mesons in a holographic model of QCD, *Eur. Phys. J. C* **74**, 2830 (2014).
- [25] E. D'Hoker and D. Z. Freedman, Supersymmetric gauge theories and the AdS/CFT correspondence, in *Theoretical Advanced Study Institute in Elementary Particle Physics (TASI 2001): Strings, Branes and EXTRA Dimensions* (2002), pp. 3–158, [arXiv:hep-th/0201253](https://arxiv.org/abs/hep-th/0201253).
- [26] L. Cappiello, O. Catà, and G. D'Ambrosio, The hadronic light by light contribution to the $(g - 2)_\mu$ with holographic models of QCD, *Phys. Rev. D* **83**, 093006 (2011).
- [27] P. Colangelo, F. De Fazio, J. J. Sanz-Cillero, F. Giannuzzi, and S. Nicotri, Anomalous AV^*V vertex function in the soft-wall holographic model of QCD, *Phys. Rev. D* **85**, 035013 (2012).
- [28] P. Colangelo, F. Giannuzzi, and S. Nicotri, π^0, η, η' two-photon transition form factors in the holographic soft-wall model and contributions to $(g - 2)_\mu$, *Phys. Lett. B* **840**, 137878 (2023).
- [29] F. Giannuzzi and S. Nicotri, $U(1)_A$ axial anomaly, η' , and topological susceptibility in the holographic soft-wall model, *Phys. Rev. D* **104**, 014021 (2021).
- [30] V. Pauk and M. Vanderhaeghen, Single meson contributions to the muon's anomalous magnetic moment, *Eur. Phys. J. C* **74**, 3008 (2014).
- [31] P. Roig and P. Sanchez-Puertas, Axial-vector exchange contribution to the hadronic light-by-light piece of the muon anomalous magnetic moment, *Phys. Rev. D* **101**, 074019 (2020).
- [32] V. Pascalutsa, V. Pauk, and M. Vanderhaeghen, Light-by-light scattering sum rules constraining meson transition form factors, *Phys. Rev. D* **85**, 116001 (2012).
- [33] P. Achard *et al.* (L3 Collaboration), $f_1(1285)$ formation in two photon collisions at LEP, *Phys. Lett. B* **526**, 269 (2002).
- [34] P. Achard *et al.* (L3 Collaboration), Study of resonance formation in the mass region 1400-MeV to 1500-MeV through the reaction $\gamma\gamma \rightarrow K^0_s K^\pm \pi^\mp$, *J. High Energy Phys.* **03** (2007) 018.
- [35] J. Leutgeb and A. Rebhan, Hadronic light-by-light contribution to the muon $g-2$ from holographic QCD with massive pions, *Phys. Rev. D* **104**, 094017 (2021).
- [36] M. Hoferichter and P. Stoffer, Asymptotic behavior of meson transition form factors, *J. High Energy Phys.* **05** (2020) 159.
- [37] J. Bijnens, E. Pallante, and J. Prades, Analysis of the hadronic light by light contributions to the muon $g-2$, *Nucl. Phys.* **B474**, 379 (1996).
- [38] M. Hayakawa, T. Kinoshita, and A. I. Sanda, Hadronic light by light scattering contribution to muon $g-2$, *Phys. Rev. D* **54**, 3137 (1996).
- [39] J. Leutgeb, J. Mager, and A. Rebhan, Hadronic light-by-light contribution to the muon $g-2$ from holographic QCD with solved $U(1)_A$ problem, *Phys. Rev. D* **107**, 054021 (2023).
- [40] A. E. Radzhabov, A. S. Zhevlakov, A. P. Martynenko, and F. A. Martynenko, Light-by-light contribution to the muon anomalous magnetic moment from the axial-vector mesons exchanges within the nonlocal quark model, *Phys. Rev. D* **108**, 014033 (2023).
- [41] E. Katz, A. Lewandowski, and M. D. Schwartz, Tensor mesons in AdS/QCD, *Phys. Rev. D* **74**, 086004 (2006).
- [42] S. Mamedov, Z. Hashimli, and S. Jafarzade, Tensor meson couplings in AdS/QCD, *Phys. Rev. D* **108**, 114032 (2023).
- [43] C. Germani and A. Kehagias, Higher-spin fields in brane-worlds, *Nucl. Phys.* **B725**, 15 (2005).
- [44] W. de Paula, T. Frederico, H. Forkel, and M. Beyer, Dynamical AdS/QCD with area-law confinement and linear Regge trajectories, *Phys. Rev. D* **79**, 075019 (2009).
- [45] Z. Abidin and C. E. Carlson, Gravitational form factors of vector mesons in an AdS/QCD model, *Phys. Rev. D* **77**, 095007 (2008).
- [46] T. Gutsche, V. E. Lyubovitskij, I. Schmidt, and A. Vega, Dilaton in a soft-wall holographic approach to mesons and baryons, *Phys. Rev. D* **85**, 076003 (2012).
- [47] V. E. Lyubovitskij and I. Schmidt, Bulk-to-boundary propagators with arbitrary total angular momentum J in soft-wall AdS/QCD, *Phys. Rev. D* **108**, 054030 (2023).
- [48] S. J. Brodsky, G. F. de Teramond, H. G. Dosch, and J. Erlich, Light-front holographic QCD and emerging confinement, *Phys. Rep.* **584**, 1 (2015).
- [49] E. Witten, Anti-de Sitter space and holography, *Adv. Theor. Math. Phys.* **2**, 253 (1998).
- [50] V. A. Novikov, M. A. Shifman, A. I. Vainshtein, and V. I. Zakharov, Are all hadrons alike?, *Nucl. Phys.* **B191**, 301 (1981).
- [51] T. M. Aliev and M. A. Shifman, Old tensor mesons in QCD sum rules, *Phys. Lett.* **112B**, 401 (1982).
- [52] C. Ewerz, M. Maniatis, and O. Nachtmann, A model for soft high-energy scattering: Tensor pomeron and vector odderon, *Ann. Phys. (Amsterdam)* **342**, 31 (2014).
- [53] M. Masuda *et al.* (Belle Collaboration), Study of π^0 pair production in single-tag two-photon collisions, *Phys. Rev. D* **93**, 032003 (2016).
- [54] G. A. Schuler, F. A. Berends, and R. van Gulik, Meson photon transition form-factors and resonance cross-sections in e^+e^- collisions, *Nucl. Phys.* **B523**, 423 (1998).
- [55] R. L. Workman *et al.* (Particle Data Group), Review of particle physics, *Prog. Theor. Exp. Phys.* **2022**, 083C01 (2022).
- [56] I. Danilkin and M. Vanderhaeghen, Light-by-light scattering sum rules in light of new data, *Phys. Rev. D* **95**, 014019 (2017).